

Baseline Probabilities for the Seasonal Prediction of Meteorological Drought

BRADFIELD LYON, MICHAEL A. BELL, AND MICHAEL K. TIPPETT*

International Research Institute for Climate and Society, Columbia University, Palisades, New York

ARUN KUMAR

NOAA/NCEP/Climate Prediction Center, Camp Springs, Maryland

MARTIN P. HOERLING AND XIAO-WEI QUAN

NOAA/Earth System Research Laboratory, Boulder, Colorado

HUI WANG

NOAA/NCEP/Climate Prediction Center, Camp Springs, Maryland

(Manuscript received 5 July 2011, in final form 6 December 2011)

ABSTRACT

The inherent persistence characteristics of various drought indicators are quantified to extract predictive information that can improve drought early warning. Predictive skill is evaluated as a function of the seasonal cycle for regions within North America. The study serves to establish a set of baseline probabilities for drought across multiple indicators amenable to direct comparison with drought indicator forecast probabilities obtained when incorporating dynamical climate model forecasts. The emphasis is on the standardized precipitation index (SPI), but the method can easily be applied to any other meteorological drought indicator, and some additional examples are provided. Monte Carlo resampling of observational data generates two sets of synthetic time series of monthly precipitation that include, and exclude, the annual cycle while removing serial correlation. For the case of no seasonality, the autocorrelation (AC) of the SPI (and seasonal precipitation percentiles, moving monthly averages of precipitation) decays linearly with increasing lag. It is shown that seasonality in the variance of accumulated precipitation serves to enhance or diminish the persistence characteristics (AC) of the SPI and related drought indicators, and the seasonal cycle can thereby provide an appreciable source of drought predictability at regional scales. The AC is used to obtain a parametric probability density function of the future state of the SPI that is based solely on its inherent persistence characteristics. In addition, a method is presented for determining the optimal persistence of the SPI for the case of no serial correlation in precipitation (again, the baseline case). The optimized, baseline probabilities are being incorporated into Internet-based tools for the display of current and forecast drought conditions in near-real time.

1. Introduction

A unique definition of drought remains elusive because the impacts of drought are both location specific

and sector specific. However, an essential feature of drought is prolonged, deficient precipitation relative to the expected climate. This feature is the basis for precipitation-based meteorological drought indices, which integrate precipitation variability over some time period. Varying time periods are considered (3, 6, 12 months, etc.) in an attempt to capture multiple aspects of land surface hydrology such as soil moisture at different depths, streamflow, and so on that are affected by precipitation variability on different time scales (Heim 2002; Svoboda et al. 2002).

The cumulative, time-integrated nature of meteorological drought events (hereinafter, simply “drought”) results in considerable persistence from one month to the

* Additional affiliation: Center of Excellence for Climate Change Research, Department of Meteorology, King Abdulaziz University, Jeddah, Saudi Arabia.

Corresponding author address: Dr. Bradfield Lyon, International Research Institute for Climate and Society, 61 Route 9W, P.O. Box 1000, Columbia University, Palisades, NY 10964-8000.
E-mail: blyon@iri.columbia.edu

next, characteristics that are valuable for both drought monitoring and early warning (Redmond 2002; Nicholls et al. 2005; Sen and Boken 2005). The generally slow evolution of drought events heightens the importance of real-time monitoring for drought early warning and prediction. A fundamental opportunity for improved drought prediction is therefore to better quantify the probability for drought conditions at a future time given that drought conditions have occurred in the immediate past—that is, to better understand drought persistence. For example, various autoregressive models have been developed that explicitly incorporate the autocorrelation (and other statistical properties) of a given drought index in their design (e.g., Sen and Boken 2005; Mishra and Desai 2005; Loaiciga and Leipnik 1996; Kendall and Dracup 1992).

Here we develop a method to quantify the baseline predictive skill for multiple drought predictors. In the absence of skillful precipitation forecasts or any knowledge of regional drought persistence characteristics more generally, improved drought prediction can nonetheless be realized through this approach. Consider the example of using a dynamical-model seasonal forecast to predict the 6-month standardized precipitation index (SPI6; McKee et al. 1993). A seasonal (i.e., 3 month) forecast of SPI6 would thus involve a forecast of seasonal precipitation that is combined with the prior 3 months of observed precipitation. For example, a 0-lead forecast made at the end of June of SPI6 (i.e., covering the period April–September) will be based on the observed precipitation for April–June and the forecast precipitation for July–September. An accurately monitored prior state of precipitation, together with a precise knowledge of the seasonal cycle of climatological precipitation, will thereby contribute to a skillful drought prediction, even when information on seasonal anomalies in future precipitation is absent. Of course, it is expected that precipitation forecasts in some regions will benefit from the prior observations through interactions among the land surface, atmosphere, and ocean (Lyon and Dole 1995; Myoung and Nielsen-Gammon 2010; Koster et al. 2010; Quan et al. 2006).

To establish a *baseline* of predictability, here we address the skill of drought index predictions solely on the basis of the persistence characteristics of those indices together with knowledge of a region's climatological seasonal cycle of precipitation variability. Again, the inherent time scales of variation in drought indices are assumed to be representative of temporal variations in different physical characteristics of land hydrology and soils and thus are expected to be both physically and practically meaningful. Having quantified this persistence, one can then quantify any additional skill provided by incorporating dynamical model precipitation forecasts that are conditioned upon

particular initialized states of the atmosphere, oceans, and land surface. Such an analysis is undertaken in a companion paper (Quan et al. 2012).

In this paper we first quantify the persistence characteristics of various drought indices that are solely attributable to their design and are independent of any knowledge of the climatological seasonal cycle of precipitation. We focus primarily on the SPI, although some additional meteorological drought indicators are also considered. We next examine how the seasonality of precipitation modifies drought persistence characteristics. The predictive “skill” associated with the inherent persistence of various drought indicators is assessed as a function of location and initial month for the domain of North America. Probability distributions of future values of a drought indicator, on the basis of persistence alone, are calculated, and we demonstrate that the inherent persistence characteristics of drought indicators can be further optimized to enhance predictive skill. In a companion paper (Quan et al. 2012) we investigate the importance of external forcing (SST and initial land surface condition) and initialization of atmospheric conditions in predicting the seasonal evolution of drought; that is, we quantify the extent to which additional forecast information can improve upon the inherent persistence of drought indicators.

The outline of the paper is as follows. In section 2 we describe the datasets used and the basic methodological approaches. The persistence characteristics, with and without seasonality taken into account, are provided in section 3. Use of persistence in providing the baseline predictive skill of the SPI is described in section 4 along with a discussion of how to modify the method to optimize that skill. An overall summary and the main conclusions of the study are described in section 5.

2. Data and method

The observationally based precipitation datasets used include the Global Precipitation Climatology Center (GPCC; Rudolf and Schneider 2005; Schneider et al. 2011) monthly gridded analyses for the globe at 0.5° latitude \times 0.5° longitude spatial resolution (1901–2007), the unified U.S.–Mexico gridded precipitation (1948–2011) at 1.0° latitude \times 1.0° longitude spatial resolution (Higgins et al. 2000; Chen et al. 2008), and the U.S. climate division data obtained from archives at the National Climatic Data Center (1895–2009; Guttman and Quayle 1996). The climate division Palmer Z index (Palmer 1965) is also utilized. The SPI was computed following the method described in Guttman (1999). In essence, the SPI computation involves first computing the cumulative probability of accumulated precipitation (over 3-, 6-, 12-month periods, etc.) at a particular location

and then transforming those cumulative probabilities to those of a standard normal distribution, $N(0, 1)$. Here we examine accumulation periods of 3, 6, 9, and 12 months, hereinafter referred to as SPI3, SPI6, and so on.

The persistence of the SPI (and a few other indices shown in section 3) is quantified through the use of Monte Carlo resampling. This resampling is done to generate two types of synthetic precipitation time series: one for which seasonality of monthly precipitation was removed and the other for which it was retained. In both sets of synthetic series the random sampling eliminates¹ any month-to-month autocorrelation (AC) in precipitation. We purposely remove the monthly AC in the synthetic time series, because our goal is to quantify the persistence characteristics of the drought indicators that result solely from their design, thus establishing a baseline for predictability. The elimination of seasonality in the synthetic precipitation time series is accomplished by concatenating 1200 randomly selected monthly values of observed precipitation *taken from any month* during the period 1900–2009 to create a time series that is 100 yr in length. That is, in this first approach the data selected for any given month are not required to follow chronologically from the previously selected month of the year. A randomly selected value for March, for example, could be followed by a randomly selected value for September, or any other month of the year. An ensemble of 100 such synthetic time series was generated in this fashion using the climate division data.

The second set of synthetic time series retained seasonality by randomly sampling across the 110 observations available for each calendar month while retaining calendar order. For example, a synthetic time series starting in January would consist of a randomly selected, observed value of January precipitation from the 110 Januarys between 1900 and 2009, then a randomly selected value for February, one for March, and so on. For the analysis over North America, a similar Monte Carlo approach was taken by randomly sampling monthly precipitation values taken from the GPCC data. In that case, it was found that an ensemble of thirty 100-yr synthetic time series was sufficient to provide robust estimates of the median value of the AC.

3. Persistence characteristics of meteorological drought indicators

a. Ignoring seasonality of precipitation

The first step was to compute the AC of various SPI indicators at different lag times ranging from 1 to 12 months

¹ The AC in any given synthetic time series may not be identically zero because of sampling. For this reason, 100 synthetic time series were generated to be able to place confidence limits on the results obtained.

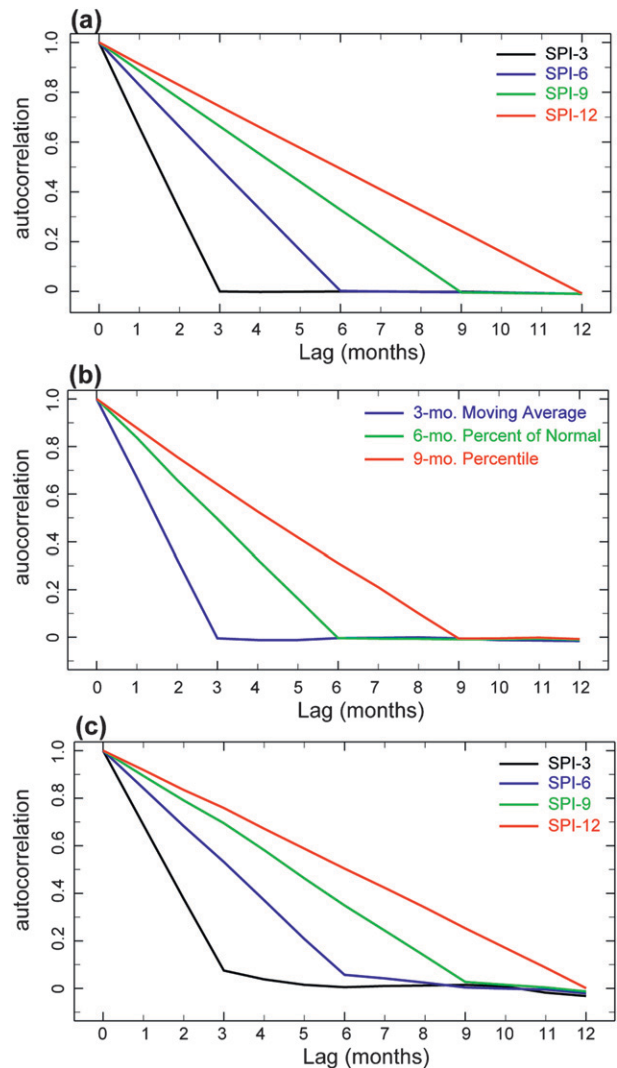


FIG. 1. Correlograms showing the median value of the AC across all 10 New York climate divisions for (a) four SPI indices in the case of no seasonality in synthetic, monthly precipitation time series; (b) three additional precipitation-based indicators that are based on the same precipitation data as in (a); and (c) four SPI indices that are based on the observed monthly precipitation for New York climate divisions during the period 1980–2010.

using the 100 synthetic climate division precipitation time series without seasonality. A correlogram representing the median values of the AC for SPI3, SPI6, SPI9, and SPI12 is shown in Fig. 1a evaluated over all 10 climate divisions in the state of New York. The AC is seen to drop off in a linear fashion with lag for each index, reaching a value of roughly zero when the time lag exceeds the accumulation period of the index. For example, the AC of the SPI3 reaches zero at a lag of 3 months, that for SPI6 reaches zero at 6 months, and so on. A linear decay of the AC for a time series of a moving average process has been described previously in the time series analysis literature

for the case of a stationary time series and serially uncorrelated data (e.g., Box and Jenkins 1976; Kedem 1993). To briefly review, consider an n -month moving average of a time series of random, monthly precipitation values P_i :

$$S_i = \frac{1}{n}[P_i + P_{i-1} + P_{i-2} + \dots + P_{i-(n-1)}], \quad (1)$$

where S_i is the average value of precipitation ending at time i and n is the number of months in the moving average. If $\text{Var}(P_i) = \sigma^2$, then an assumption that each month's precipitation is independent and has the same variance gives that $\text{Var}(S_i) = \sigma^2/n$, and the covariance between any two adjacent values in the moving average is $\text{Cov}(S_i, S_{i-1}) = \sigma^2(n-1)/n^2$ such that the 1-month lag autocorrelation is given by $\rho_{S_i, S_{i-1}} = (n-1)/n$. The right-hand side of this last expression is simply the fraction of common variance in the moving average (in the case of the SPI, the respective n -month accumulations of precipitation) at 1-month lag. In a similar way, the correlation at a lag of l months is $\rho_{S_i, S_{i-l}} = (n-l)/n$, for $l \leq n$. Thus, the AC at 1-month lag for SPI3 is $2/3$ (0.67) and for SPI12 it is $11/12$ (0.92); at 2-month lag these respective values are $1/3$ (0.33) and $10/12$ (0.83), and so on.

Because seasonality has purposely been ignored in these first examples, the above results do not depend either on the mean or variance of the precipitation and will thus hold for any region. Two time series with different means and variances, for example, can nonetheless be perfectly correlated. For each climate division the synthetic precipitation time series without seasonality is just a sequence of random numbers bounded by the range of observed precipitation over the 110 yr in that division. A random number generator would produce the same results regardless of the underlying distribution of the data (e.g., normal vs a gamma distribution). Further, the above relationships (i.e., a linear decrease in AC with lag) will hold for other indices that are based on accumulated precipitation such as the percent of median of n -month precipitation, percentiles of n -month precipitation, a 90-day moving average of precipitation, and so on (see Fig. 1b). For regions in which the observed climate shows little seasonality of precipitation (and small autocorrelation in monthly precipitation), these results will approximately hold in the observations. One such example is shown in Fig. 1c, which displays the median AC across climate divisions in the state of New York on the basis of observed precipitation for the period 1980–2010. Note that all of the correlograms in Fig. 1 suggest substantial predictive “skill” out to several months lead time depending on the index considered (e.g., the SPI12 has an AC of ≈ 0.75 at 3-month lead time).

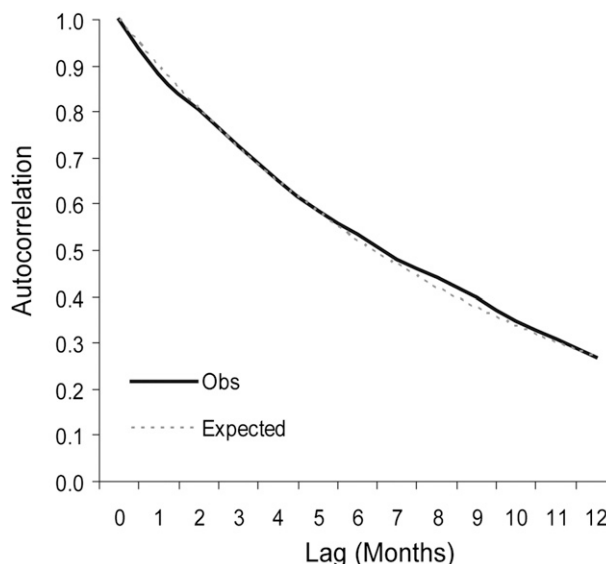


FIG. 2. As in Fig. 1, but for the PDSI for the case of no seasonality or serial correlation in monthly values of the Palmer Z index. The dashed line indicates the expected AC given the PDSI index formulation.

The Palmer drought severity index (PDSI) is based on a recursive formula that includes the so-called monthly Z index (Palmer 1965):

$$\text{PDSI}_i = 0.897 \times \text{PDSI}_{i-1} + Z_i/3, \quad (2)$$

where PDSI_i and Z_i are the values of the PDSI and Z index at month i , respectively, the Z_i term being a function of both monthly temperature and precipitation. The PDSI was an early attempt to create a meteorological drought index on the basis of a surface water balance method. A number of issues have been raised concerning the representativeness of regional and seasonal variations in the PDSI with respect to observed conditions (e.g., Alley 1984), but it is used here only as an example of an index with high persistence characteristics. For the case of no seasonality in precipitation and temperature (and zero AC of the Z index), the last term on the right-hand side of Eq. (2) essentially represents white noise. As such, the AC of the PDSI is only dependent on the first term. Hence, the AC of the PDSI for the case of no seasonality will be expected to drop off roughly as $(0.897)^l$, where l is the time lag in months. For the U.S. climate division data, the Z index was scrambled in a manner similar to what was done for precipitation, leading to the generation of 100 synthetic time series 100 yr in length for both the case in which seasonality is omitted and in which it is retained. An example showing the median AC of the PDSI for the case of no seasonality is shown in Fig. 2, again evaluated across the 10 climate divisions in the

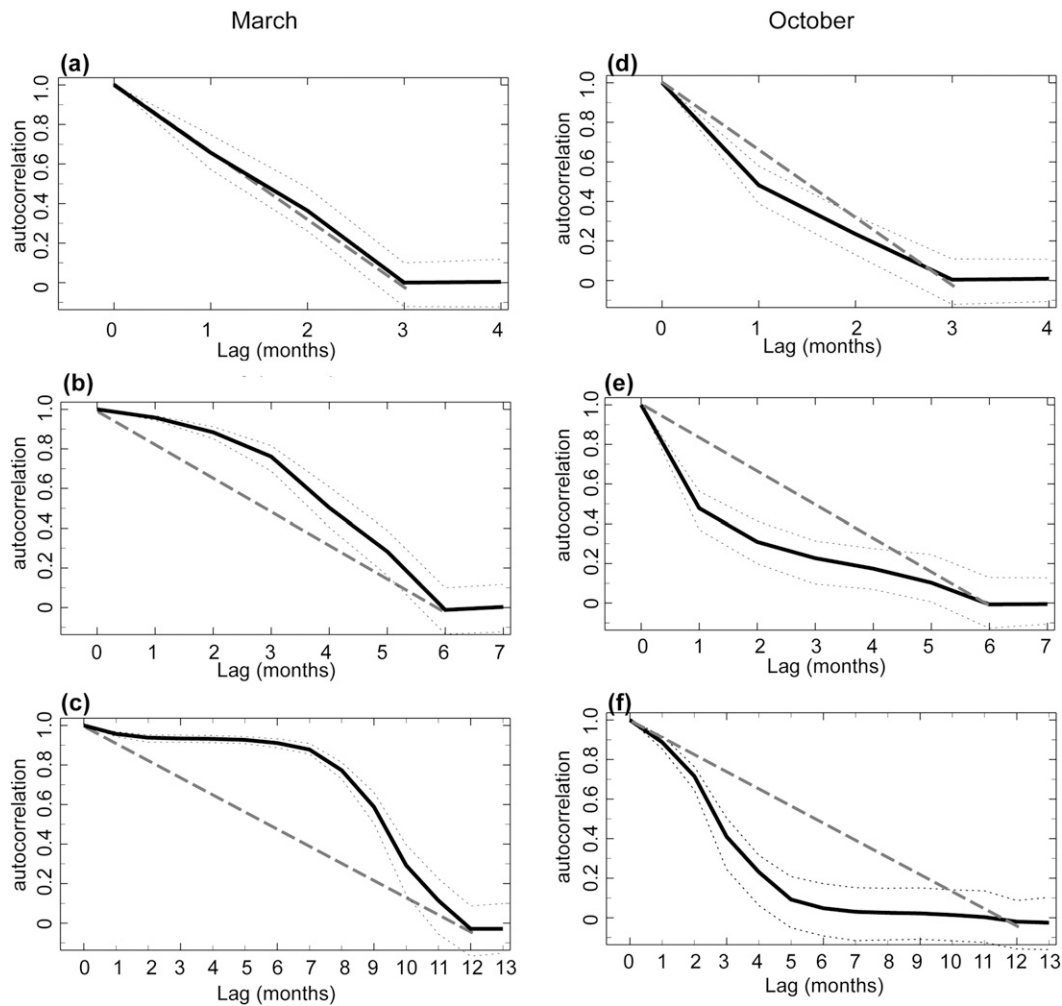


FIG. 3. Correlograms showing the median value of the AC of different SPI indices across all climate divisions in California as obtained from the synthetic time series that include seasonality in monthly precipitation for (left) a March and (right) an October start time: (a),(d) SPI3, (b),(e) SPI6, and (c),(f) SPI12. The thin dotted lines in each of the plots indicate the 5th and 95th percentile limits on the AC. The straight, dashed lines indicate the AC for the case of no seasonality.

state of New York. For such a case, the AC is indeed observed to drop off in a manner that is consistent with a priori expectations.

b. Including seasonality of precipitation

Obviously seasonality in precipitation is an important characteristic of local climate at many locations. The results from the previous section thus primarily serve as a benchmark for comparison with subsequent examples for the case in which seasonality is retained. An example of the important role that seasonality of monthly precipitation plays in the persistence of various SPI indices is shown in Fig. 3 for the case of the California climate divisions (chosen because of the large annual cycle in precipitation there). The 100 synthetic time series of

randomly sampled monthly precipitation with seasonality retained were used to generate the correlograms presented in Fig. 3 for the SPI3, SPI6, and SPI12 for start times of March and October. These plots show the median value of the AC computed across all 100 synthetic time series. In addition, the 95% confidence limits on the AC (dotted lines in Fig. 3) were obtained by ranking the AC values across the 100 time series for a given lag time. For reference, the straight, dashed lines in Fig. 3 show the autocorrelation of the various indices for the case of no seasonality (i.e., a linear decay in AC with increasing lag).

For the case of the March start time and in which seasonality of precipitation is retained (Fig. 3, left column), the median values of the AC for the SPI6 and SPI12 are seen to remain higher than for the case with no seasonality for

several months. For SPI3 this tendency is less pronounced. As shown in appendix A, the effect of seasonality on the persistence characteristics of the SPI (or other indices that are based on the temporal integration of precipitation) is through the *variability* of the accumulated amount of precipitation over a particular time period (6 months, 12 months, etc.). There is no dependence of the drought index AC on the seasonality of the mean precipitation, but rather only on its variance. For example, March is near the end of the precipitation season in California. As such, both the total amount of precipitation received in subsequent months (April, May, June, etc.) and its variability are small when compared with that typically received in the earlier months of January–March. Thus, when multimonth accumulated precipitation totals are considered (e.g., as when computing SPI6), the post-March period contributes little to the variability of the total whereas the pre-March months contribute the most. The majority of the variance in 6-month precipitation is then associated with precipitation in the earlier period, leading to a substantial AC in the SPI between March and subsequent boreal spring and summer months. In observations, the variance in accumulated precipitation increases roughly in proportion to the total precipitation received. This can be seen graphically in Fig. 4, which contrasts the seasonality of 6-month precipitation totals and associated variability in California versus New York. For New York, the 6-month accumulated precipitation does not vary substantially from one overlapping 6-month period to the next, with relatively small changes in the standard deviation as well. By contrast, in California the accumulated precipitation amount varies considerably depending on what part of the calendar year is considered, with the standard deviation seen to behave in a similar fashion. For a March start time (Fig. 4a), the precipitation totals and variability in California decrease with increasing lag.

An October start time in California is near the start of the main precipitation season. Multimonth precipitation totals (and associated variability) will therefore typically increase rapidly in the months following October relative to those months prior (Fig. 4b); thus, the “memory” of the relative dry season is quickly lost and the AC drops off quickly. Indeed, as seen in the plots in the right-hand column of Fig. 3 the decay of the AC in this case is even faster than for a linear decrease associated with no seasonality in precipitation. Thus, if the AC of the SPI6 is used as a measure of its predictability, then seasonality is seen both to enhance and to reduce that predictability depending on the seasonality of precipitation variance. Put another way, if *drought* conditions exist at the start of the climatological dry season at a particular location, they are not going to be ameliorated during the dry season when

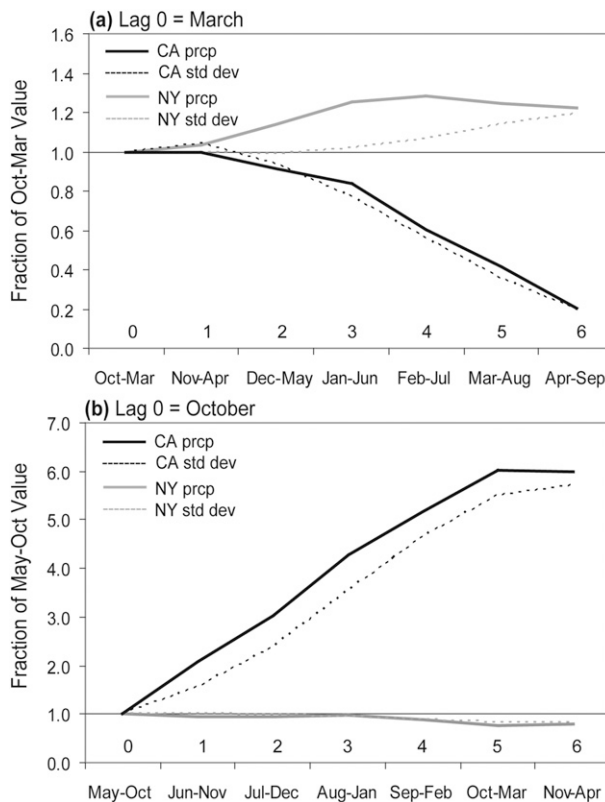


FIG. 4. The fraction of (a) October–March and (b) May–October precipitation (solid lines) and standard deviation (dashed lines) for subsequent, overlapping 6-month periods. The black (gray) lines represent values averaged across all climate divisions in CA (NY). The thin horizontal lines in both plots are the fractional values for the case of no seasonality in either variable (i.e., unity). The numbers along the abscissa represent lag times relative to March in (a) and October in (b).

variability is relatively small (in climatological terms). On the other hand, the beginning of the precipitation season with its greater variability provides the next opportunity to break a drought (as defined by multimonth precipitation totals).

The AC of the PDSI was also considered for the case in which precipitation seasonality is retained. For this calculation, the climate division Z-index values were randomly sampled over the 110-yr observational period but, as in the case for precipitation, were sampled for sequential calendar months so as to include seasonality. Results for California are shown in Fig. 5, again for March and October start times. For reference, the PDSI AC decay rate for the case of no seasonality [given as $(0.897)^t$] is also displayed. The results are reminiscent of those obtained for the SPI6 and SPI12, with higher AC values than for the no-seasonality case for the March start time and lower relative values for the October start time. The inherent time scale of variation of the PDSI in California

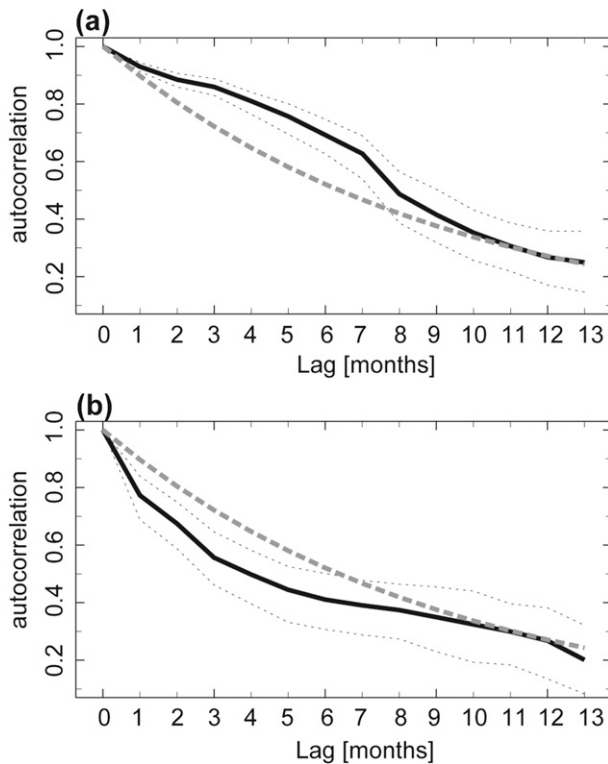


FIG. 5. As in Fig. 3, but for the median value of AC of the PDSI across all climate divisions in California for (a) March and (b) October start times.

thus corresponds roughly to that associated with the SPI evaluated over a time period between 6 and 12 months. From an applications perspective it is highly desirable to match the characteristic time scale of the SPI (or any drought index) to that of a particular variable of interest (shallow vs deep soil moisture, streamflow, etc.).

c. Spatial variations in persistence characteristics

The geographical and seasonal variations in the persistence characteristics of the SPI3, SPI6, and SPI12 indices for North America for the case in which precipitation seasonality is retained were also evaluated, with representative results shown in Figs. 6–8 for four start times (March, June, September, and December). The results are based on synthetic time series that include seasonality generated from the GPCC data from the period 1908–2007. Persistence in Figs. 6–8 is defined as the number of consecutive months that the autocorrelation exceeds 0.6. This AC threshold was subjectively chosen since 1) it represents a value with high statistical significance (significance factor $p < 0.01$) and 2) from a practical viewpoint a correlation of 0.6 indicates that more than one-third of the variance is explained (in a linear regression sense). On this latter point, for 100 yr of data a correlation coefficient

of $r = 0.2$ is found to be statistically significant at $p < 0.05$ (on the basis of a two-tailed t test), but such a correlation would only be associated with an explained variance of 4%, rendering the results much less actionable (i.e., 96% of the variance is attributable to unpredictable sources). For reference, Fig. 9 shows the seasonal fraction of annual precipitation for each start time to provide a measure of the seasonality in precipitation. If there is no seasonality in precipitation, the fraction of annual precipitation during any 3-month season will be 25%. Shading in Fig. 9 thus delineates values higher and lower than this percentage as a function of the 3-month season considered.

For locations where there is little annual cycle to precipitation (such as the eastern United States), the persistence characteristics in Figs. 6–8 are seen to be similar regardless of the start time, as expected. Also expected is that persistence is generally greater for larger accumulation periods of the SPI, with no location in North America showing persistence exceeding 1 month (by the definition used here) for the SPI3, for example. In regions with a pronounced annual cycle in precipitation variance, there are pronounced variations in the persistence characteristics as a function of start time. For example, when comparing the geographical variations in persistence with the seasonal cycle shown in Fig. 9, it is not surprising that the greatest persistence occurs near the beginning of comparative dry seasons across all three SPI indicators. For instance, much of the west coast of the United States and Canada shows strong persistence from March initial conditions. In the U.S. Southwest and northwestern Mexico, the influence of the North American monsoon is evident. The U.S. and Canadian plains show substantial persistence from a September initial condition relative to other seasons. Also note that the persistence may be substantial at many locations. The SPI6, for example, may have AC exceeding 0.6 for as many as 4 months; for SPI12, it can reach 9 months in some locations. As discussed previously, for a start time near the beginning of the climatological precipitation season, persistence is lower. The west coast of the United States for a September start time is a salient example.

In actual observations persistence can, of course, vary from the baseline values because of feedbacks between the land surface and atmosphere, persistence from SST forcing (e.g., ENSO), and so on. To let one gain a sense of how large the difference can be, Fig. 10 shows the number of consecutive months that the AC of the SPI6 exceeds 0.6 for four different start times on the basis of actual observations (from the GPCC dataset). This figure can be directly compared with the baseline case shown in Fig. 7. By this measure, we see that the actual persistence exceeds the baseline values at several locations but that the difference is typically on the order of 1 month.

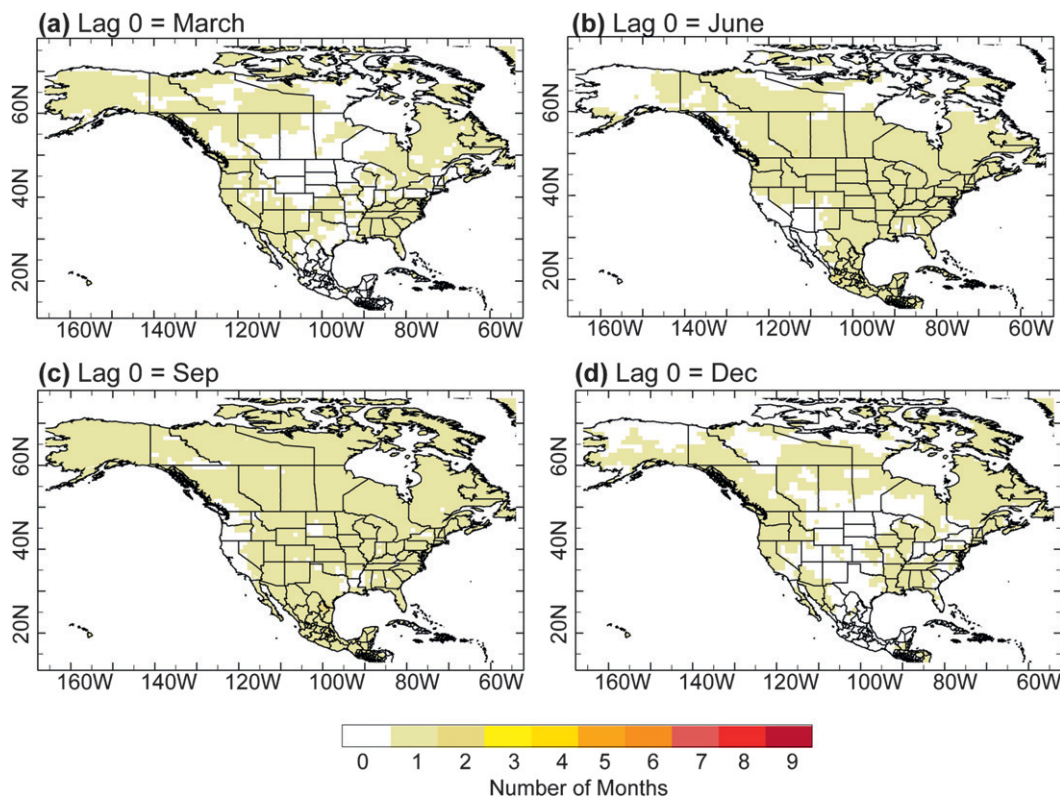


FIG. 6. Geographical distribution of the number of consecutive months in which the median AC of the SPI3 exceeds 0.6 for start times of (a) March, (b) June, (c) September, and (d) December. All plots are based on a set of thirty 100-yr synthetic time series of monthly values of gridded precipitation derived from the GPCC dataset in which seasonality is retained.

It is clear that the often substantial persistence of drought indicators has important predictive information once the initial drought state has been determined. Developing such baseline drought probabilities in a prediction setting is described in the next section, focusing solely on variations of the SPI. A similar approach could just as well be used to construct similar baseline probabilities for any other meteorological drought index, including those that include the effects of both precipitation and evaporative fluxes (such as the PDSI).

4. Baseline probabilities for meteorological drought prediction

a. Computing baseline probability distributions

The results from the previous section show that the inherent persistence of drought indicator values can provide useful predictive information—in some cases, out to several months. This predictive skill was assessed by considering the AC value of the SPI at various lag times. The focus of this section is to show how such persistence characteristics can be further utilized to determine the

full probability density function (pdf) of the SPI at various lead times given any initial drought index condition (i.e., initial SPI value). These pdfs provide baseline probabilities because, again, we are only considering the inherent persistence characteristics of drought indicators.

The pdf of future values of the SPI (or other drought indices) that are based on persistence can be determined in various ways. For example, given the initial value of the SPI, an empirical approach can be used to generate a plume of future SPI values by using historical observations of monthly precipitation for subsequent months. This is essentially the method used in ensemble streamflow (or “seasonal”) prediction (Day 1985). Building a reliable pdf, however, requires a substantial number of observations, although additional techniques could be applied to “smooth” the results from this nonparametric approach, such as implementing a kernel density estimator.

An alternative, parametric approach is to use the mean value of the SPI plume described above (obtained from the climatological mean precipitation value) and to compute the lag AC of the SPI. The AC can then be used to determine the full pdf of SPI values at different lead times

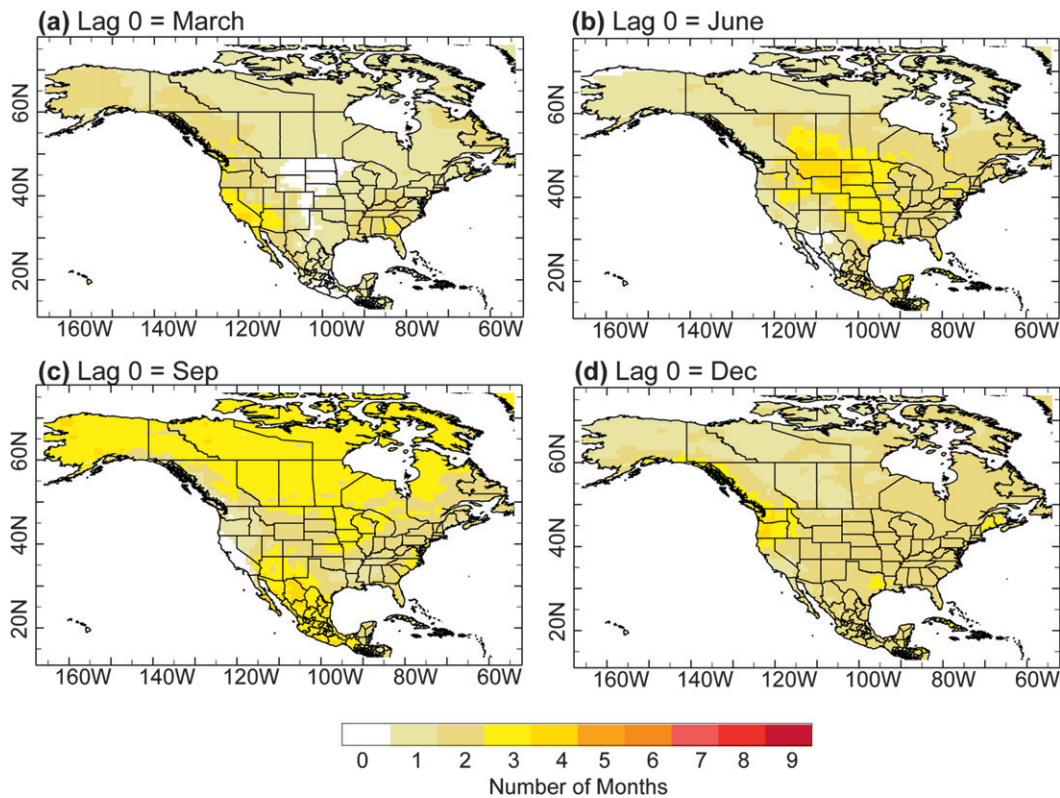


FIG. 7. As in Fig. 6, but for the SPI6.

analytically. By design, the SPI follows a normal distribution with unit variance. Following the example of seasonal climate forecasts (Tippett et al. 2007), the standard deviation of the forecast value of the SPI pdf can then be estimated as

$$\sigma_{\text{fcst}(l)} = (1 - \rho_l^2)^{1/2}, \quad (3)$$

where ρ_l is the AC for the l th lead time. Because in the current case any predictive skill of the SPI results solely from knowledge of its initial condition, the signal will be completely lost for lead times beyond the accumulation period of the index (as shown previously). There may, however, still be useful information contained in the knowledge of the initial SPI condition out to several months of lead time depending on the index used and start time considered. An example is shown in Fig. 11 for the lower Hudson Valley New York climate division (division 5) on the basis of an initial SPI9 value of -0.88 observed in March of 1999. The pdfs of SPI9 at 1-month lags from the March start time are plotted in Fig. 11, which indicates that the dispersion at short lead times is less than that at longer leads given the greater memory of the initial condition [higher AC of the SPI in Eq. (3)]

in the former case. At increasing lead times, the pdf of the SPI9 tends toward its climatological distribution, which after 9 months is simply $N(0, 1)$. At 4-month lead (July of 1999), the observed value of the SPI9 at this location was -1.06 . Note that, relative to the climatological mean, the unconditional persistence “forecast” for July of 1999 indicates an enhanced probability of SPI9 values being < -1.0 .

b. Computing the “optimal” persistence of drought indicators

The last example shows how the baseline probabilities of the SPI, obtained only from the persistence characteristics of the index, its initial value, and climatological precipitation, exhibit some predictive skill. While valuable, the level of skill in this general treatment can be improved with some modification to the method. Because we are only considering skill associated with persistence (and the case of no serial correlation in monthly precipitation), the predictive signal is fully contained in the initial drought state. In the case of the SPI (and related indices), however, the signal resides solely in the monthly precipitation values that are common to the index at the initial and subsequent times. Using the AC

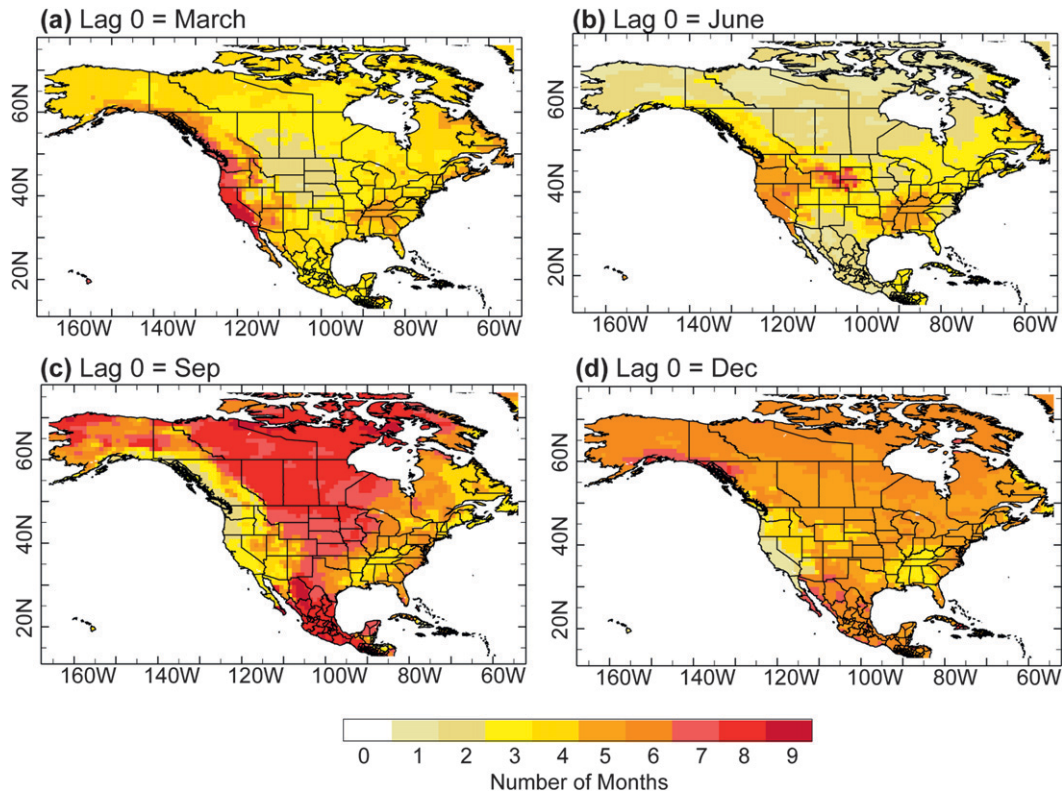


FIG. 8. As in Fig. 6, but for the SPI12.

of the SPI is thus less than optimal for determining the maximum predictive skill.

Consider the schematic in Fig. 12a, which shows the monthly precipitation values used in computing the SPI6 at a given time t and 3 months later ($t + 3$). The three months of common information contain the signal, and the other months represent noise added to that signal. Thus, when correlating SPI6(t) with SPI6($t + 3$), there are three months of noise in the initial condition [the first three months of precipitation used in computing the SPI6(t)] that are going to dilute the common signal and reduce the correlation. The three months of noise contained in SPI6 ($t + 3$) cannot be avoided (again, we are considering the case of no serial correlation in monthly precipitation). As shown in appendix B, the correlation may be increased when using only the months of common information in the initial condition in the calculation. In the current example (see Fig. 12b), the SPI3(t) is a better predictor of SPI6($t + 3$) than is SPI6(t). For SPI6($t + 4$), the best predictor will be SPI2(t), and so on. In mathematical terms, for the case of no seasonality in monthly precipitation it was shown previously that the AC of the SPI n goes as $(n - l)/n$, where l is the lag in months and n is the number of months of accumulated precipitation in the SPI. From appendix B, the optimal correlation instead goes as

$$\{1 + [l/(n - l)]\}^{-1/2} \approx [n - (l/2)]/n, \quad (4)$$

where l is again the lag and n is the months of precipitation of the SPI n being predicted. The difference between methods is shown in Fig. 13a for the case of no seasonality and in Figs. 13b and 13c for the California climate divisions where seasonality is included. As shown in the figure, the differences in correlation between the two methods can be substantial and, depending on the seasonality of precipitation variability, the improvement in skill can actually *increase* with increasing lag when using the optimal persistence method. It is clear that when drought index predictions are based solely on persistence characteristics the optimal persistence method is the preferred approach.

c. Displaying probabilistic drought indicator information

Once the full pdf of the SPI has been determined, the information it contains can be displayed in a variety of ways. One example is to evaluate the probability that the index will fall below (or above) some selected threshold. This probability is determined from the cumulative distribution function for a normal distribution:

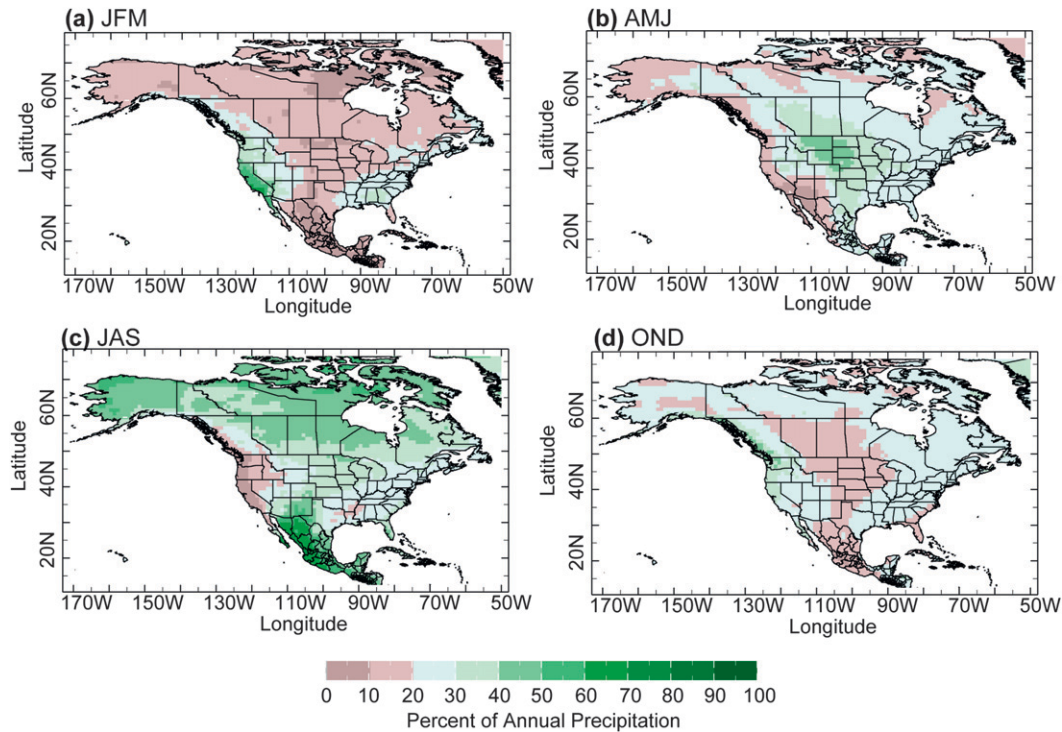


FIG. 9. Seasonal fraction of annual precipitation (expressed as a percent) for (a) January–March, (b) April–June, (c) July–September, and (d) October–December from the GPCC data for 1971–2000.

$$P_r(X \leq x) = \frac{1}{2} \left[1 + \operatorname{erf} \left(\frac{x - \mu_{\text{fcst}}}{\sqrt{2}\sigma_{\text{fcst}}} \right) \right], \quad (5)$$

where $P_r(X \leq x)$ is the probability of the SPI being below the value x and μ_{fcst} and σ_{fcst} are again the mean and standard deviation of the forecast of the SPI at a given lead time. For drought concerns, the probability that the index is less than a specific trigger threshold (Steinemann and Cavalcanti 2006) may be of particular interest, for example. Conversely, it may be of interest to know what the expected value of the index will be at a given probability level and lead time.

Another application is to examine the marginal distribution of the index, which indicates the value of the index expected to be exceeded only $n\%$ of the time. Again, this will clearly depend on the initial condition of the index and a specified lead time. In mathematical terms, the marginal value of the SPI n having probability P may be computed by rewriting Eq. (5) as

$$x = \mu_{\text{fcst}} + \sqrt{2}\sigma_{\text{fcst}} \operatorname{erf}^{-1}(2P - 1), \quad (6)$$

where μ_{fcst} for a lead time l from an initial time t is given by $\rho(t + l)\text{SPI}(t)$ and σ_{fcst} is the standard deviation of the forecast SPI at lead time l . Here, P is the marginal

distribution probability level and erf^{-1} is the inverse of the error function [the latter being defined in terms of the integral of the Gaussian probability density function for $N(0, 1)$].

Given the initial condition of a drought indicator and the derived, unconditional pdfs of their subsequent evolution, the results can be displayed in a number of ways. Some examples are shown in Fig. 14. Figure 14a shows the initial condition of the SPI12 in April of 2011. The probability that the July 2011 SPI12 will be < -1.0 is shown in Fig. 14b, with the best-estimate value of the SPI12 at the end of July of 2011 (based only on its unconditional persistence) shown in Fig. 14c. The observed SPI12 for July of 2011 is shown in Fig. 14d.

The approach outlined here, in which the persistence characteristics of a drought indicator are used to make probabilistic assessments of future values of the indicator, represents a generalization of the basic method reported by Karl et al. (1987). The latter study only considered the climatological probability of receiving the amount of precipitation necessary to ameliorate drought conditions, as based on the PDSI. Here, Internet-based tools are being developed that will compute the probability of exceeding any desired threshold of multiple drought indicators at multiple lead times, as just one example.

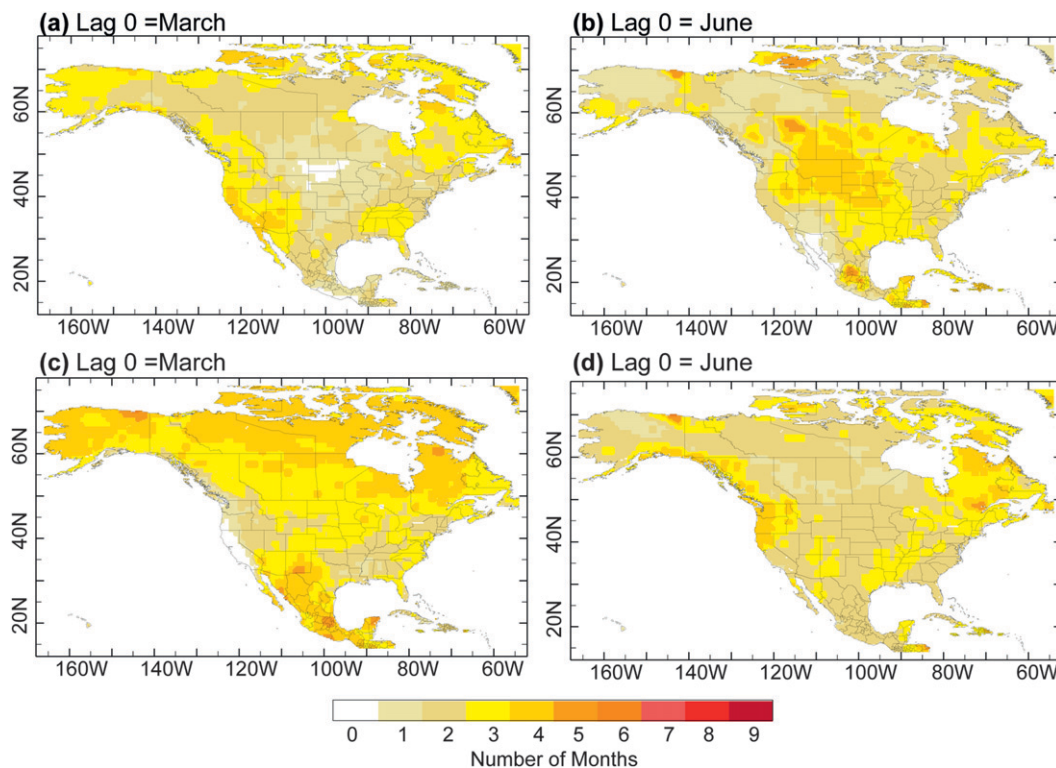


FIG. 10. As in Fig. 7, but for the SPI6 on the basis of observed precipitation.

5. Summary and conclusions

The inherent persistence of drought makes possible potentially useful predictive information out to several months of lead time. Here, a method is developed to quantify the persistence characteristics of various drought indicators 1) to extract predictive information of the evolution of these indicators and 2) to establish a set of baseline probabilities for drought across multiple indicators that can be compared with forecast probabilities obtained from dynamical climate model predictions. The primary focus here is on the SPI, but the method could easily be applied to any other meteorological drought indicator.

A Monte Carlo approach was used to examine persistence characteristics. In this approach, ensembles of synthetic time series are generated by concatenating randomly sampled, observed values. Two sets of synthetic time series were generated, one in which precipitation seasonality was removed and the other in which it was retained. For the case of no seasonality and for indices such as the SPI, seasonal precipitation percentiles, and moving averages of monthly precipitation, the AC of the indicators is seen to decay linearly with increasing lag. The SPI12, for example, has an AC of 0.67 (8/12) at 4-month lag and 0.33 (4/12) at 8-month lag. In locations with a small annual cycle in precipitation variability, such as the northeastern United States, a linear decay in AC is

seen in actual observations as well. Given the recursive design of the PDSI, in the case of no seasonality in its associated monthly Z index, the AC decreases exponentially with lag.

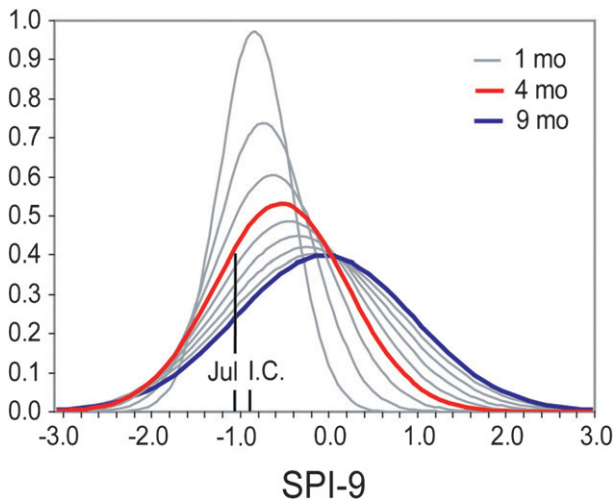


FIG. 11. The pdfs of the SPI9 at 1-month lags (gray lines) from a start time of March 1999 for a climate division in the Hudson Valley of New York. The red line indicates the pdf at 4 months of lead time (July 1999), and the blue line shows the pdf for 9 months of lead time (December 1999). The initial condition (I.C.) for March 1999 is indicated at the bottom of the plot, as is the observed value for July 1999.

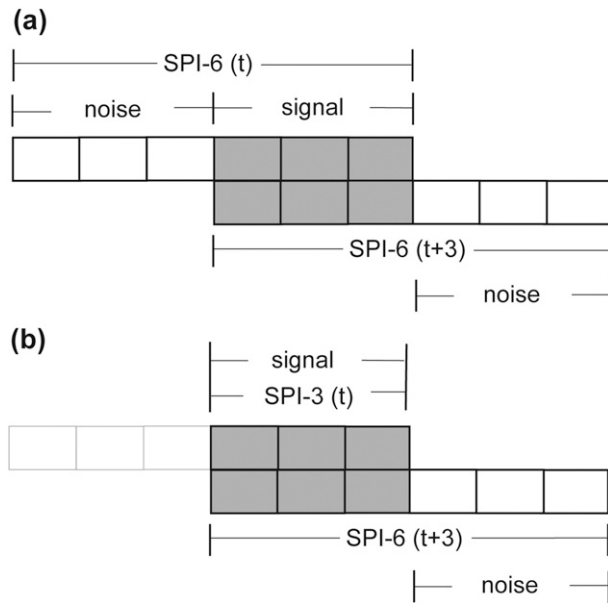


FIG. 12. (a) Schematic view of monthly precipitation values for two overlapping 6-month periods (ending at time t and at time $t + 3$ months) used for computing the SPI6. The shaded (white) boxes indicate common monthly values of precipitation (“noise”). (b) Using only the common months in the initial condition reduces such noise in the common signal. Thus, SPI3(t) captures more of the common signal of the initial condition than does SPI6(t).

We have shown that seasonality in precipitation variance can appreciably enhance (or diminish) the predictive skill derived from drought indicator persistence, with substantial variations depending on location and season considered. In locations with a strong annual cycle, persistence of the SPI is enhanced (reduced) when the initial drought condition considered occurs at the end (beginning) of the precipitation season. Thus, the annual cycle in precipitation variance can both increase and decrease the inherent predictability of the SPI depending on the season and location considered. In addition, it has been shown that, regardless of regional seasonality, the inherent persistence of drought indicators is maximized when utilizing only the common months of information when computing lagged correlations. This is referred to as the “optimal persistence” in this baseline context.

Baseline probabilities of drought index values were computed using a parametric approach that incorporates the AC of the index to generate the full pdf of future index values. This was done for multiple time periods and lead times for the SPI. Once the full pdf has been obtained, the information it contains can provide a variety of practical information. Examples include mapping the best-estimate value of a drought index at various lead times, plotting the probability of exceeding a selected

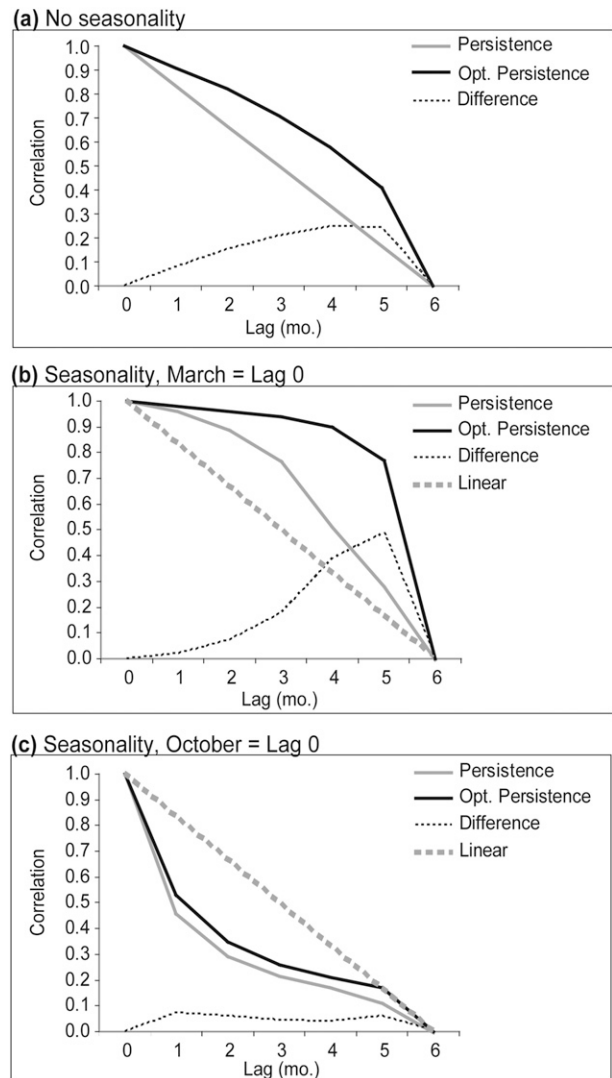


FIG. 13. (a) Lagged correlations of the SPI6 for the case of no seasonality in precipitation using the standard approach (gray line) vs the optimal persistence method (solid black line). The thin dashed line shows the difference between correlation values. (b) As in (a), but for the case including seasonality with results averaged across all California climate divisions for a March start time. The thick dashed line indicates a linear decay (i.e., the case of no seasonality). (c) As in (b), but for an October start time.

value of the index at that lead time, or plotting the value of the index associated with the marginal distribution at a given probability. Internet-based tools are currently being developed that will display this information in near-real time to generate baseline forecasts. The associated baseline probabilities will serve as benchmark values for comparison with predictions of various drought indicators that incorporate seasonal precipitation forecasts from dynamical climate models. Those comparisons are provided in a companion paper (Quan et al. 2012).

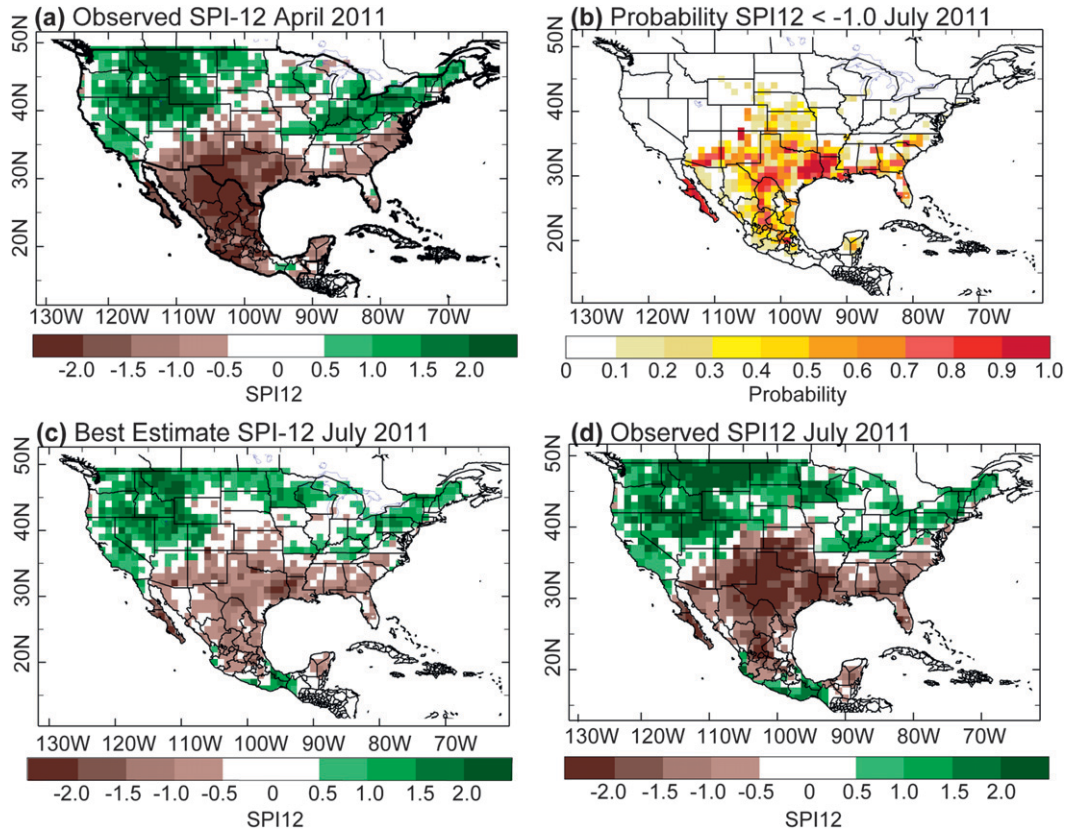


FIG. 14. (a) The observed value of the SPI12 for April 2011. (b) The probability of the SPI12 being < -1.0 in July 2011. (c) The best estimate of the SPI12 for July 2011. (d) The observed SPI12 for July 2011. All plots are based on the U.S.–Mexico unified precipitation dataset.

Acknowledgments. We are grateful to Benno Blumenthal, director of the IRI Data Library, for his assistance with some of the computations and to the reviewers for their helpful comments. This work was supported by National Oceanic and Atmospheric Administration Grant NA08OAR4310622.

APPENDIX A

The Effect of Seasonality on Persistence

Define S_i as the n -month accumulated precipitation ending with month i . Then,

$$S_i = P_i + P_{i-1} + \dots + P_{i-n+1},$$

and its value l months in the future is

$$S_{i+l} = P_{i+l} + P_{i+l-1} + \dots + P_{i+l-n+1}.$$

What is the correlation between S_i and S_{i+l} ? We assume that the monthly precipitation values P_i are

uncorrelated. Therefore, any correlation between S_i and S_{i+l} is due entirely to the monthly precipitation values that appear in both sums. For $l < n$, S_i and S_{i+l} have $n - l$ common terms, which are convenient to denote by

$$C_{il} = P_i + P_{i-1} + \dots + P_{i-n+l+1}.$$

Denoting the terms that are not in common, that is, “disjoint” terms, by

$$D_{il} = P_{i-n+l} + \dots + P_{i-n+1} \quad \text{and}$$

$$D'_{il} = P_{i+l} + \dots + P_{i+1},$$

we can write

$$S_i = C_{il} + D_{il} \quad \text{and} \quad S_{i+l} = C_{il} + D'_{il}.$$

The correlation between S_i and S_{i+l} is

$$\text{cor}(S_i, S_{i+l}) = \frac{\text{cov}(S_i, S_{i+l})}{\sigma(S_i)\sigma(S_{i+l})}. \tag{A1}$$

Using the standard linearity property of covariance, we can write

$$\begin{aligned}\text{cov}(S_i, S_{i+1}) &= \text{cov}(C_{il}, C_{il}) + \text{cov}(C_{il}, D'_{il}) \\ &\quad + \text{cov}(C_{il}, D_{il}) + \text{cov}(D_{il}, D'_{il}) \\ &= \sigma^2(C_{il}),\end{aligned}$$

where $\text{cov}(C_i, D_i) = \text{cov}(C_i, D'_i) = \text{cov}(D_i, D'_i) = 0$ follows from the independence of the monthly precipitation values. Another consequence of the independence of the monthly precipitation values is that $\sigma^2(S_i) = \sigma^2(C_{il}) + \sigma^2(D_{il})$ and, likewise, $\sigma^2(S_{i+1}) = \sigma^2(C_{il}) + \sigma^2(D'_{il})$. Substitution of these results into Eq. (1) gives

$$\text{cor}(S_i, S_{i+1}) = \left\{ \left[1 + \frac{\sigma^2(D_{il})}{\sigma^2(C_{il})} \right] \left[1 + \frac{\sigma^2(D'_{il})}{\sigma^2(C_{il})} \right] \right\}^{-1/2}.$$

The form of the above expression shows that the effect of seasonality is that as the variance of the disjoint term increases (decreases) relative to the variance of the common terms, the correlation decreases (increases). In the case of no seasonality, the variances of C_{il} , D_{il} , and D'_{il} are proportional to the number of terms they contain, and

$$\frac{\sigma^2(D_{il})}{\sigma^2(C_{il})} = \frac{\sigma^2(D'_{il})}{\sigma^2(C_{il})} = \frac{l}{n-l},$$

it then follows that

$$\text{cor}(S_i, S_{i+1}) = \left[\left(1 + \frac{l}{n-l} \right)^2 \right]^{-1/2} = \frac{n-l}{n}.$$

APPENDIX B

The Optimal Persistence of Drought Indicators

Note that the best predictor of S_{i+1} given S_i is not S_i . The reason for this is that S_i contains a contribution from D_{il} , which we have assumed is uncorrelated with S_{i+1} (see Fig. 12 in the main text). Instead, the best predictor is the conditional mean:

$$\text{Mean}(S_{i+1} | S_i) = C_{il} + \text{mean}(D'_{il}).$$

The correlation of the conditional mean with S_{i+1} is

$$\text{cor}(C_{il}, S_{i+1}) = \left[1 + \frac{\sigma^2(D'_{il})}{\sigma^2(C_{il})} \right]^{-1/2},$$

which is strictly greater than $\text{cor}(S_i, S_{i+1})$ for $\sigma^2(D_{il}) > 0$. The dependence of $\text{cor}(C_{il}, S_{i+1})$ on seasonality is simple—it decreases as the future variance $\sigma^2(D'_{il})$ increases relative to the observed variance $\sigma^2(C_{il})$. In the case of no seasonality,

$$\text{cor}(C_{il}, S_{i+1}) = \{1 + [l/(n-l)]\}^{-1/2} \approx [n - (l/2)]/n.$$

REFERENCES

- Alley, W. M., 1984: The Palmer drought severity index: Limitations and assumptions. *J. Climate Appl. Meteor.*, **23**, 1100–1109.
- Box, G. E. P., and G. M. Jenkins, 1976: *Time Series Analysis: Forecasting and Control*. Rev. ed., Holden-Day, 575 pp.
- Chen, M., W. Shi, P. Xie, V. B. S. Silva, V. E. Kousky, R. Wayne Higgins, and J. E. Janowiak, 2008: Assessing objective techniques for gauge-based analyses of global daily precipitation. *J. Geophys. Res.*, **113**, D04110, doi:10.1029/2007JD009132.
- Day, G. N., 1985: Extended streamflow forecasting using NWSRFS. *J. Water Resour. Plan. Manage.*, **111**, 157–170.
- Guttman, N. B., 1999: Accepting the standardized precipitation index: A calculation algorithm. *J. Amer. Water Resour. Assoc.*, **35**, 311–322.
- , and R. G. Quayle, 1996: A historical perspective of U.S. climate divisions. *Bull. Amer. Meteor. Soc.*, **77**, 293–303.
- Heim, R. R., 2002: A review of twentieth-century drought indices used in the United States. *Bull. Amer. Meteor. Soc.*, **83**, 1149–1165.
- Higgins, W., W. Shi, E. Yarosh, and R. Joyce, 2000: *Improved United States Precipitation Quality Control System and Analysis*. NCEP/Climate Prediction Center Atlas 7, 40 pp.
- Karl, T. R., F. Quinlan, and D. Z. Ezell, 1987: Drought termination and amelioration: Its climatological probability. *J. Climate Appl. Meteor.*, **26**, 1198–1209.
- Kedem, B., 1993: *Time Series Analysis by Higher Order Crossings*. IEEE Press, 318 pp.
- Kendall, J. R., and D. A. Dracup, 1992: On the generation of drought events using an alternating renewal-reward model. *Stochastic Hydrol. Hydraul.*, **6**, 55–68.
- Koster, R. D., and Coauthors, 2010: Contribution of land surface initialization to subseasonal forecast skill: First results from a multi-model experiment. *Geophys. Res. Lett.*, **37**, L02402, doi:10.1029/2009GL041677.
- Loaiciga, H. A., and R. B. Leipnik, 1996: Stochastic renewal model of low-flow streamflow sequences. *Stochastic Hydrol. Hydraul.*, **10**, 65–85.
- Lyon, B., and R. M. Dole, 1995: A diagnostic comparison of the 1980 and 1988 U.S. summer heat wave–droughts. *J. Climate*, **8**, 1658–1675.
- McKee, T. B., N. J. Doesken, and J. Kliest, 1993: The relationship of drought frequency and duration to time scales. Preprints, *Eighth Conf. of Applied Climatology*, Anaheim, CA, Amer. Meteor. Soc., 179–184.
- Mishra, V. R., and A. K. Desai, 2005: Drought forecasting using stochastic models. *Stochastic Environ. Res. Risk Assess.*, **19**, 326–339.
- Myoung, B., and J. W. Nielsen-Gammon, 2010: The convective instability pathway to warm season drought in Texas. Part I: The role of convective inhibition and its modulation by soil moisture. *J. Climate*, **23**, 4461–4473.

- Nicholls, N., M. J. Coughlan, and K. Monnik, 2005: The challenge of climate prediction in mitigating drought impacts. *Drought and Water Crises, Science Technology, and Management Issues*, D. A. Wilhite, Ed., Taylor and Francis, 33–51.
- Palmer, W. C., 1965: Meteorological drought. U.S. Dept. of Commerce Weather Bureau Research Paper No. 45, 65 pp. [Available online at <http://www.ncdc.noaa.gov/temp-and-precip/drought/docs/palmer.pdf>.]
- Quan, X. W., M. P. Hoerling, J. S. Whitaker, G. T. Bates, and T. Y. Xu, 2006: Diagnosing sources of U.S. seasonal forecast skill. *J. Climate*, **19**, 3279–3293.
- , —, B. Lyon, A. Kumar, M. Bell, M. Tippet, and H. Wang, 2012: Prospects for dynamical prediction of meteorological drought. *J. Appl. Meteor. Climatol.*, **51**, 1238–1252.
- Redmond, K., 2002: The depiction of drought—A commentary. *Bull. Amer. Meteor. Soc.*, **83**, 1143–1147.
- Rudolf, B., and U. Schneider, 2005: Calculation of gridded precipitation data for the global land-surface using in-situ gauge observations. *Proc. Second Workshop of the Int. Precipitation Working Group*, Monterey, CA, EUMETSAT, 231–247.
- Schneider, U., A. Becker, A. Meyer-Christoffer, M. Ziese, and B. Rudolf, 2011: Global precipitation analysis products of the GPCC. Deutscher Wetterdienst Global Precipitation Climatology Centre Rep., 13 pp. [Available online at ftp://ftp-anon.dwd.de/pub/data/gpcc/PDF/GPCC_intro_products_2008.pdf.]
- Sen, Z., and V. K. Boken, 2005: Techniques to predict agricultural droughts. *Monitoring and Predicting Agricultural Drought*, V. K. Boken, A. P. Cracknell, and R. L. Heathcote, Eds., Oxford University Press, 40–54.
- Steinemann, A. C., and L. F. N. Cavalcanti, 2006: Developing multiple indicators and triggers for drought plans. *J. Water Resour. Plan. Manage.*, **132**, 164–174.
- Svoboda, M., and Coauthors, 2002: The drought monitor. *Bull. Amer. Meteor. Soc.*, **83**, 1181–1190.
- Tippett, M. K., A. G. Barnston, and A. W. Robertson, 2007: Estimation of seasonal precipitation tercile-based categorical probabilities from ensembles. *J. Climate*, **20**, 2210–2228.